AN ALTERNATIVE GABOR FILTERING SCHEME

Adams Wai-Kin Kong

Forensic and Security Laboratory, School of Computer Engineering,
Nanyang Technological University, Nanyang Avenue, Singapore, 639798.
E-mail: adamskong@ntu.edu.sg

ABSTRACT

An elementary function that is now commonly referred to as Gabor filter was derived from uncertainty relation for information by Gabor to overcome the representation limit of Fourier analysis. For image-based applications (e.g. biometric recognition), researchers amend the weights of Gabor filters to produce zero DC (direct current) Gabor filters. This amendment can significantly change the shape of Gabor filters, when they use a special range of parameters. The aim of this paper is to develop a new Gabor filtering scheme to overcome this problem. Two different types of zero DC Gabor filters are compared with the proposed scheme on face recognition. FERET database is employed in the experiments. The Gabor phase from the proposed filtering scheme gives improvement in the range between 11% and 8.5%, and the performance of its magnitude is comparable with other schemes.

Index Terms— Filtering, Interpolation, Image processing

1. INTRODUCTION

To break the representation limit of Hitherto communication theory that describes signals either in time domain or Fourier domain, Gabor proposed a method of analyzing signals in which time and frequency information can be captured simultaneously. This method was especially designed for the signals having finite duration and whose frequencies very with time (e.g., sound) [1]. It is constituted by three fundamental components, uncertainty relation for information, elementary functions that are now generally referred to as Gabor functions, Gabor filters and Gabor wavelets, and an algorithm for computing decomposition coefficients. The uncertainty relation for information said that for any function, the product of its effective width in time domain and its effective width in frequency domain is limited by an infimum $1/2$ [1]. Based on the uncertainty relation for information, Gabor discovered that an elementary function,

$$g_1(t) = \exp(-0.5(t-\mu)^2/\sigma^2)\exp(iwt), \qquad (1)$$

where σ controls the resolution of the analysis and μ and w are the positions of the function in time and frequency domains, respectively, reaches the theoretical limit. Given a signal f, Gabor attempted to decompose f in terms of the elementary functions (i.e., $f \approx \sum_j c_j g_j$), where g_js are the elementary functions with different parameters and c_js are the corresponding coefficients [1]. This decomposition approach is called Gabor expansion. Since the elementary functions are not orthogonal, several algorithms were proposed to compute the Gabor expansion coefficients [2-3].

Gabor was interested in Gabor expansion for one-dimensional signals, whereas since 1980, the two-dimensional (2D) versions of the elementary functions (called 2D Gabor filters) have been extensively used as convolution filters, which was motivated by the research results in biological vision systems. 2D Gabor filters have been regarded as an important tool for a variety of image processing and pattern recognition problems (e.g. biometric recognition). A 2D Gabor filter in spatial domain is defined as

$$g(x,y) = \exp\{-\pi[x'^2a^2 + y'^2b^2]\} \times \exp\{-2\pi i[u_0x' + v_0y']\}, \qquad (2)$$

where $x' = (x-x_0)\cos\alpha + (y-y_0)\sin\alpha$ and $y' = -(x-x_0)\sin\alpha + (y-y_0)\cos\alpha$ [4]. There are seven degrees of freedom in 2D Gabor filters: (x_0, y_0) is the center of the filter in spatial domain, $\omega_0 = \sqrt{u_0^2 + v_0^2}$ is the spatial frequency, $\tan^{-1}(v_0/u_0)$ is the relative orientation between the complex wave and the Gaussian function, a and b control the shape of the Gaussian function and α is the orientation of the Gaussian function. Fig. 1 shows a Gabor filter. Without loss of generality, in the rest of this paper, (x_0, y_0) is set to (0, 0) and α is also set to 0. To eliminate the influence of the power of Gabor filter, a normalized Gabor filter, $g_n = g/\|g\|$ is commonly used. Its spatial filtering outputs, phase and magnitude are

$$P_1(I, g_n) = \tan^{-1}\frac{\iint I(x,y)g_{ni}(x,y)dxdy}{\iint I(x,y)g_{nr}(x,y)dxdy}, \qquad (3)$$

$$M_1(I, g_n) = \sqrt{\left[\iint I(x,y)g_{ni}(x,y)dxdy\right]^2 + \left[\iint I(x,y)g_{nr}(x,y)dxdy\right]^2}, \qquad (4)$$

where I is a 2D signal; g_{nr} and g_{ni} represent the real and imaginary parts of the Gabor filter g_n. For convenience, g_n is used to denote $g_n(x, y)$. The same notations are employed for other symbols.

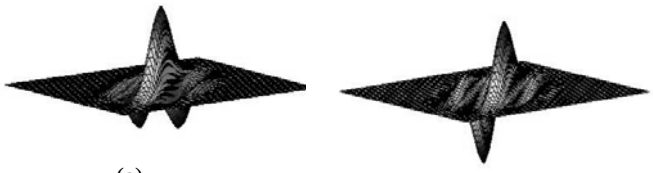

(a) (b)

Fig. 1 (a) The real part and (b) the imaginary part of a Gabor filter

In many image-based applications, variation of DC components generally deteriorates systems performance. To deal with this problem, researchers commonly use zero DC Gabor filters. A zero DC Gabor filter [5] can be generated by

$$g(x,y) = \exp\{-\pi[x^2a^2 + y^2b^2]\} \times (\exp\{-2\pi i[u_0x + v_0y]\} - \exp(-\pi[\frac{u_0^2}{a^2} + \frac{v_0^2}{b^2}])). \quad (5)$$

Fig. 2 shows two Gabor filters and the corresponding zero DC Gabor filters generated by Eq. 5. The first and second rows are the real and imaginary parts of the two original Gabor filters, respectively and the third row is the real parts of the zero DC Gabor filters. Fig. 2 does not include the imaginary parts of the zero DC Gabor filters because Eq. 5 amends real parts only. This figure demonstrates that the shape of Gabor filters can be modified significantly by the redistributed filter weights, especially when the number of cycles of the complex wave in the Gaussian function is few.

A recent paper [6] shows that under some conditions, the Gabor filter can be used to detect the corresponding Gabor atom, which is defined as

$$Z(x,y) = \frac{A_Z}{\|g\|}\exp(-\pi[x^2a^2 + y^2b^2]) \times \cos(-2\pi(u_0x + v_0y) - \phi). \quad (6)$$

More precisely, the phase and magnitude defined in Eqs. 3-4 are approximated A_Z and ϕ, respectively. Using the Gabor atom as a part of a target signal and Gabor expansion, a new Gabor filtering scheme is proposed in this paper to overcome the weakness of the current zero DC Gabor filters.

The rest of this paper is organized as follows. Section 2 derives a new Gabor filtering scheme from a detection point of view. Section 3 evaluates the proposed Gabor filtering scheme on face recognition. Section 4 offers some concluding remarks.

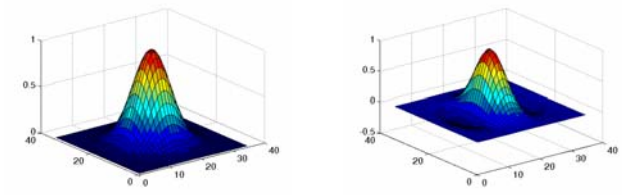

(a) (b)

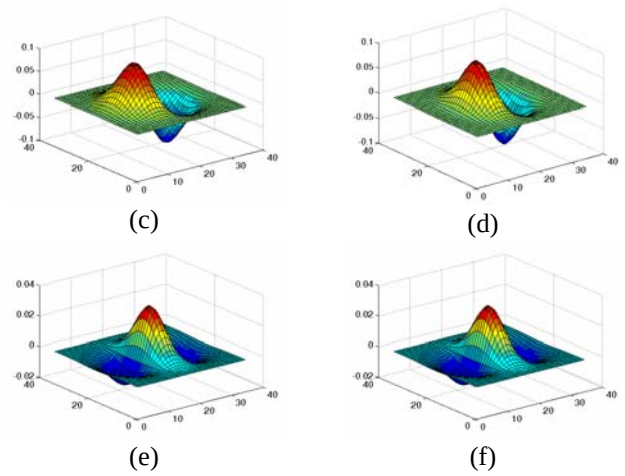

(c) (d) (e) (f)

Fig. 2 Comparison of Gabor filters and zero DC Gabor filters generated by Eq. 5. The first and second columns are two sets of Gabor filters. The first and second rows are the real and imaginary parts of Gabor filters. The third row is the real part of the corresponding zero DC Gabor filter.

2. NEW GABOR FILTERING SCHEMES DERIVED FROM GABOR EXPANSION

Originally, Gabor used the elementary functions for signal decomposition (i.e., $f \approx \sum_j c_j g_j$) [1]. Each pair of c_j and g_j was referred to one quantum of information by Gabor. If g_js are given, c_js can be computed through optimizing $E(f - \sum_j c_j g_j)$, where E is an objective function. The quanta of information depend on the parameters of Gabor filters, the number of Gabor filters, the signal and the objective function. The following subsections firstly show that the spatial filtering output of Gabor filters is in fact the coefficient, c_j in a quantum of information derived from least squares objective function and then the proposed Gabor filtering scheme is derived from Gabor expansion.

2.1. Assumptions and Notations

For clear presentation, a set of notations and assumptions is essential. Gabor filters are functions in L^2 space, i.e., $\int\int g_n \times g_n^* dxdy < \infty$, where * represents a complex conjugate and the signals considered in this paper are assumed to be real-valued functions in L^2 space. Their norms and inner product are respectively defined as $\|g_n\| = \sqrt{\int\int g_n \times g_n^* dxdy}$, $\|I\| = \sqrt{\int\int I \times I^* dxdy}$ and $< g_n, I >= \int\int g_n \times I^* dxdy$, where I is a signal. This inner product is in fact a continuous version of spatial filtering. Since I is a real-valued function in L^2 space,

$< g_n, I >= \iint g_n \times I dxdy$. Using these notations, $M_1 = |< g_n, I >|$ and $P_1 = \arg(< g_n, I >)$.

2.2. The Relationship between Gabor Expansion and Gabor Filtering

Given a Gabor filter and a signal, the coefficient c_0 in the quantum of information can be calculated from $c_0 = \arg(\min_c \|I - cg_n\|^2)$, where c is a complex number denoted as $c = c_r + ic_i$. We have $c_r = < I, g_{nr} >$ and $c_i = - < I, g_{ni} >$. If c_0 represents the information in the form, $c_0 = Me^{-i\gamma}$, we obtain $M = \sqrt{< I, g_{nr} >^2 + < I, g_{ni} >^2}$ and $\gamma = \tan^{-1} \frac{< I, g_{ni} >}{< I, g_{nr} >}$. In other words, the coefficient in the quantum of information is equivalent to the filtering output. This equivalent relationship further implies that the current Gabor filtering scheme is a special case of Gabor expansion when a single filtering output is considered.

2.3 A New Gabor Filtering Scheme

Using the previous result, a new Gabor filter is designed based on Gabor expansion. It is noted that Gabor filters have representation power solely around their filter centers, while the least squares objective function in Section 2.2 neglects positions of errors. Furthermore, it does not handle the DC component in the signal explicitly. To respond to these two new considerations, a new Gabor filtering scheme is proposed in this subsection, especially for image-based applications. Its corresponding Gabor expansion is formulated as $\hat{c}_0 = \arg\left(\min_{\hat{c}} \left\| \sqrt{G}\, \mathrm{Re}(I - \hat{c} g_n - d u_u) \right\|^2 \right)$, where $d \in \Re$, G is a real even weighting function with respect to the center of g_n, $u_n = u / \|u\|$ and u is defined as

$$u(x,y) = \begin{cases} 1 \; if \; (x,y) \; is \; in \; the \; signal \; domain \\ 0 \; otherwise \end{cases} . \quad (7)$$

$$\left\| \sqrt{G}\, \mathrm{Re}(I - \hat{c} g_n - d u_n) \right\|^2 = \left\| \sqrt{G} (I - \hat{c}_r g_{nr} + \hat{c}_i g_{ni} - d u_n) \right\|^2 \quad (8)$$

$$\approx < GI, I > -2\hat{c}_r < I, Gg_{nr} > +2\hat{c}_i < I, Gg_{ni} > -2d < GI, u_n > \\ +2\hat{c}_r d < Gg_{nr}, u_n > +\hat{c}_r^2 < Gg_{nr}, g_{nr} > +\hat{c}_i^2 < Gg_{ni}, g_{ni} > +d^2 < Gu_n, u_n > \quad (9)$$

Eq. 9 is an approximation of Eq. 8 because $< Gu_n, g_{ni} > \neq 0$. If the distance between the center of g_n and the boundary of the signal domain is longer than three standard deviations of the Gaussian function of g_n, $< Gu_n, g_{ni} > \approx 0$. Computing partial derivatives of $\left\| \sqrt{G}\, \mathrm{Re}(I - \hat{c} g_n - d u_u) \right\|^2$, we can obtain

$$\hat{c}_r = \frac{< I, Gg_{nr} >< Gu_n, u_n > - < Gg_{nr}, u_n >< I, Gu_n >}{< Gg_{nr}, g_{nr} >< Gu_n, u_n > - < Gg_{nr}, u_n >^2}, \quad (10)$$

$$\hat{c}_i = \frac{- < I, Gg_{ni} >}{< Gg_{ni}, g_{ni} >}, \quad (11)$$

$$d = \frac{< Gg_{nr}, g_{nr} >< I, Gu_n > - < I, Gg_{nr} >< Gg_{nr}, u_n >}{< Gg_{nr}, g_{nr} >< Gu_n, u_n > - < Gg_{nr}, u_n >^2}. \quad (12)$$

Finally, the magnitude and phase of this Gabor filtering scheme are defined as

$$P_2(I, g_n) = \tan^{-1}\left(\frac{(< Gg_{nr}, g_{nr} >< Gu_n, u_n > - < Gg_{nr}, u_n >^2) < I, Gg_{ni} >}{(< I, Gg_{nr} >< Gu_n, u_n > - < Gg_{nr}, u_n >< I, Gu_n >) < Gg_{ni}, g_{ni} >} \right), \quad (13)$$

$$M_2(I, g_n) = \sqrt{\left(\frac{< I, Gg_{nr} >< Gu_n, u_n > - < Gg_{nr}, u_n >< I, Gu_n >}{< Gg_{nr}, g_{nr} >< Gu_n, u_n > - < Gg_{nr}, u_n >^2} \right)^2 + \left(\frac{< I, Gg_{ni} >}{< Gg_{ni}, g_{ni} >} \right)^2}. \quad (14)$$

The Gaussian function of g_n is a natural choice for the weighting function G because it reflects the importance of the approximation errors at different locations. Fig. 3 illustrates the usefulness of the weighting function. Fig. 3(a) is constituted by three signals, two Gaussian signals and one Gabor atom. $\mathrm{Re}(\hat{c} g_n + d u_u)$ is used to approximate the Gabor atom. Fig. 3(b) employs no weighting function, while Fig. 3(c) is the result of using the Gaussian function as the weighting function. Fig. 3(b) shows that the coefficient d is seriously influenced by the two Gaussian signals; as a result, it is not zero. The corresponding coefficient $\hat{c}$ is also affected because these two coefficients are connected. Fig. 3(c) shows that the Gaussian weighting function effectively prevents the influence of the Gaussian signals. This figure clearly demonstrates the essentiality of the weighting function in the formulation. In the following section, the Gaussian function is employed as the weighting function and this filtering scheme is called G-Gabor filtering scheme (G-Gabor-FS).

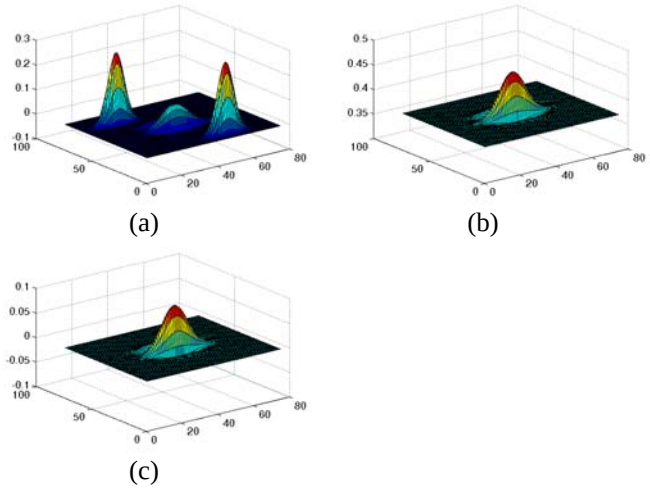

Fig. 3 Illustration of the importance of the weighting function in Eq. 8. (a) The original signal, (b) and (c) the approximations of the Gabor atom in the original signal by Eq. 8 using constant and Gaussian weighting functions, respectively.

3. EXPERIMENTS

In this section, we compare two types of zero DC Gabor filters with the proposed scheme. The first one is given in Eq. 5, and the second one is generated by redistributing the excess filter weights evenly [7]. The second approach in fact considers a Gabor filter as a finite digital filter. For the sake of convenience, the current filtering scheme using the first and second types of zero DC Gabor filters is respectively called N-Gabor-FS and L-Gabor-FS.

To quantitatively compare the three filtering schemes, they are applied to face recognition, a challenging research problem in computer vision and pattern recognition. FERET database is employed in this evaluation [8-9]. Two hundred subjects are randomly selected from it and three images of each subject are chosen from sets fa, fb and dup1. Images from set fa are considered as galleries for FERET and the others are used as probes. The eye positions are manually located for alignment. The aligned images are cropped and normalized to 128 by 128 preprocessed images.

The parameters of Gabor filters used in this study are $u_0 = 0$, b/a=2, $\alpha_p \in \{0, \pi/6, \pi/3, \pi/2, 2\pi/3, 5\pi/6\}$, $a = 1/6\sqrt{\pi}$, and $v_o = f_q\sqrt{2\pi}b/6$, where $f_q = \{0.5, 1.5, 2.5, 3.5, 4.5\}$. f_q is the number of cycles of the complex wave within 6 standard deviations at y' direction. To extract stable features, the magnitude and phase generated by the Gabor filters having maximum magnitude are used for matching. In other words, we only use features generated from g_{pq} if $M_{1(2)}(I, g_{pq}) \geq M_{1(2)}(I, g_{p_1q_1})$, where $p \neq p_1$ or $q \neq q_1$. Cosine measure, $\cos(\gamma_s(x,y) - \gamma_t(x,y))$, where $\gamma_s(x,y)$ and $\gamma_t(x,y)$ are two phases from two different images at the same position (x, y) is used for phase matching. If they are generated by two different Gabor filters, it is no reason to compare them. Thus, the cosine measure for comparing two images is defined as $\sum_{(x,y)\in\Omega} \cos(\gamma_s(x,y), \gamma_t(x,y))/n$, where Ω is a set of points that $\gamma_s(x,y)$ and $\gamma_t(x,y)$ are from the same Gabor filter and n is the number of points in Ω. Similarly, cosine measure defined as, $\frac{\sum_{(x,y)\in\Omega} m_s(x,y) \times m_t(x,y)}{\sqrt{\sum_{(x,y)\in\Omega} m_s(x,y)^2} \sqrt{\sum_{(x,y)\in\Omega} m_t(x,y)^2}}$, where $m_s(x,y)$ and $m_t(x,y)$ are two magnitudes from two images at position (x, y) is used to compare two image magnitudes. Although the eye positions are manually located, they are still not perfect. One of the features is required to translate vertically and horizontally, and then matching is performed again. Both the ranges of the vertical and the horizontal translation are –3 to 3. The maximum similarity obtained by translated matching is regarded as the final similarity measure.

Table 1 lists the accuracies and shows that G-Gabor-FS is always the best, except in case 1. This comparison points out that the recognition power of Gabor phase is seriously suppressed by the current Gabor filtering scheme for face recognition.

Table 1 The experimental results for FERET database

Case	Probe	Features	L-Gabor-FS	N-Gabor-FS	G-Gabor-FS
1	Fb	Magnitude	0.9100	0.8800	0.9050
2		Phase	0.6900	0.6950	0.7850
3	Dup1	Magnitude	0.600	0.6150	0.6150
4		Phase	0.6050	0.6300	0.7150

4. CONCLUSION

This paper pinpoints that the scheme used to remove DC component in Gabor filters can significantly change their shape. To overcome this problem, a new Gabor filtering scheme is proposed. Comparing the current and proposed Gabor filtering schemes on face recognition, the phase of G-Gabor-FS gives improvement in the range between 11% and 8.5%, and the performance of its magnitude is comparable with other schemes.

5. ACKNOWLEDGMENTS

The author thanks NIST for sharing the face images. This work is supported by Ministry of Education, Singapore.

6. REFERENCES

[1] D. Gabor, "Theory of Communication", *Journal of Inst. Electr. Engi*., vol. 93, 429-457, 1946

[2] J.G. Daugman, "Complete discrete 2-D Gabor transforms by neural networks for image analysis and compression", *IEEE TASP*, vol. 36, no. 7, pp. 1169-1179, 1988

[3] A. Ibrahim and M.R. Azimi-Sadjadi, "A fast learning algorithm for Gabor transform", *IEEE TIP*, vol. 5, no. pp. 171-175, 1996

[4] J.G. Daugman, "Uncertainty relation for resolution in space, spatial frequency, and orientation optimized by two-dimensional visual cortical filters", *Journal of Optical America A*, vol. 2, no. 7, pp. 1160-1169, 1985

[5] T.S. Lee, "Image representation using 2D Gabor Wavelets", *IEEE TPAMI*, vol. 18, no. 10, pp. 959-971, 1996

[6] A. Kong, "An analysis of Gabor detection", in Proceeding of International Conference on Image Analysis and Recognition, pp. 64-72, 2009

[7] D. Zhang, W.K. Kong, J. You and M. Wong, "On-line palmprint identification", *IEEE TPAMI*, vol. 25, no. 1041-1050, 2003

[8] P.J. Phillips, H. Wechsler, J. Huang and P. Rauss, "The FERET database and evaluation procedure for face recognition algorithms", *Image and Vision Computing*, vol. 16, no. 5, pp. 295-306, 1998

[9] P.J. Phillips, H. Moon, S.A. Rizvi and P.J. Rauss, "The FERET evaluation methodology for face recognition algorithms", *IEEE TPAMI,* vol. 22, pp. 1090-1104, 2000